J Biochem Phytomed. 2024; 3(1): 21-35. doi: 10.34172/jbp.2024.7.

JBP
Journal of Biochemicals and Phytomedicine
eISSN: 2958-8561

An *In Silico* Molecular Docking and ADMET Studies of Some GC-MS Analysed Compounds from Methanol Extract of *Mitracapus hirtus*

Abubakar Hassan [1]*, Alam Ozair [2], Tukur Mukhtar [1], Suleiman Mustapha [1], Muazu Alhaji Safiya [1], Yusuf Amina Jega [3]

[1] Department of Chemistry, Sokoto State University, Sokoto, Nigeria
[2] Department of Pharmaceutical Chemistry, Jamia Hamdard, New Delhi, India
[3] Department of Pharmaceutical and Medicinal Chemistry, Usmanu Danfodiyo University, Sokoto, Nigeria

ARTICLE INFO

Article Type:
Research

Article History:
Received: 12 Dec 2023
Revised: 16 May 2024
Accepted: 25 May 2024
Available online: 30 Jun 2024

Keywords:
Molecular Docking,
ADMET,
GC-MS,
14α DM,
Secondary metabolites

Corresponding author:
E-mail: hassan.abubakar@ssu.edu.ng

ABSTRACT

Introduction: Fungal infections, particularly in Nigeria, represent a significant public health concern and are among the most prevalent infections in Sub-Saharan Africa.

Methods: An in silico molecular docking and ADMET analysis were conducted on several GC-MS-analyzed compounds targeting two fungal enzymes—Squalene Synthase (SS) and Lanosterol-14α Demethylase (14α DM). The analyses were performed using PyRx software's AutoDock tools, SwissADME, and PROTox II.

Results: The docking analysis of seven selected compounds from the GC-MS analysis, including Methyl 3-[(3-chlorophenyl)methyl]-2-cyclohexylimidazo[1,2-a]pyridine-6-carboxylate, 4-(Phenylsulfanyl)-6-(pyrrolidin-1-yl)-2,1,3-benzoxadiazole, 2,4,6-Triphenylthiopyran, 3-(Naphthalen-1-ylmethyl)-1-pentyl-1H-indole, 5-(Benzyloxy)-1-methyl-1H-indole, 1-(2H-1,3-Benzodioxol-5-yl)-3-(7-methoxy-2H-1,3-benzodioxol-5-yl)prop-2-en-1-one, and 2-Benzo[1,3]dioxol-5-yl-8-methoxy-3-nitro-2H-chromene, revealed interactions between the selected ligands and the active sites of SS and 14α DM. The binding scores for the best poses ranged from -8.6 to -10.3 kcal/mol for SS, and from -8.7 to -9.7 kcal/mol for 14α DM. Among these, 2,4,6-Triphenylthiopyran demonstrated the highest affinity and the lowest docking score for both targets, while 5-(Benzyloxy)-1-methyl-1H-indole and 2-Benzo[1,3]dioxol-5-yl-8-methoxy-3-nitro-2H-chromene exhibited the highest docking scores against the respective target enzymes. The drug-likeness parameters and pharmacokinetic properties of the phytochemical constituents of *M. hirtus* showed molecular weights ranging from 237.30 to 382.88 g/mol, numbers of rotatable bonds from 3 to 6, H-bond donors were 0 for all test compounds, H-bond acceptors ranged from 0 to 6, iLogP values ranged from 2.87 to 4.01, TPSA values ranged from 4.93 to 82.74 Å², and molar refractivity values ranged from 74.18 to 107.82. High GI absorption, BBB permeability, P-glycoprotein substrates, inhibition of CYP1A2, CYP2C19, and CYP2C9, as well as skin permeability (LogKp), were also evaluated.

Conclusion: This study identified several compounds as potential inhibitors of SS and 14α DM demethylase, with superior binding affinity compared to co-crystallized ligands, alongside a favorable ADMET profile.

Please cite this paper as:
Hassan A, Ozair A, Mukhtar T, Mustaph S, Alhaji Safiya M, Jega YA. An *in silico* molecular docking and admet studies of some gc-ms analysed compounds from methanol extract of *Mitracapus hirtus*. Journal of Biochemicals and Phytomedicine. 2024; 3(1): 21-35. DOI: 10.34172/jbp.2024.7.

Introduction

Infections and diseases caused by fungi are a growing global public health threat. Invasive fungal diseases are a new and growing hazard to global health, which is made worse by the rapid rise of antifungal resistance and, in many contexts, restricted access to high-quality diagnoses and treatment. (Brown et al., 2012; Denning, 2022). Those having invasive procedures, getting broad- spectrum antibiotics, critically ill patients in an intensive care unit (ICU), and anyone using immune-suppressing medications are also at risk (Bongomin et al., 2017). Despite the rising concern, fungal infections receive very little attention and funding, which results in a dearth of high-quality information on the prevalence of fungal diseases and trends in antifungal resistance (WHO, 2022). Those with underlying health issues or a weaker immune system, such as those with chronic lung illness, previous tuberculosis (TB), HIV, cancer, or diabetes mellitus, are those who are most at risk (WHO, 2022). More than 1.5 million people die each year from fungi related illnesses, despite the fact that these fatalities are avoidable, diseases cause by fungi are still ignored despite this rising fatality rates, especially in developing nations (Bongomin et al., 2017). Aspergillus, Candida, Cryptococcus species, Pneumocystis jirovecii, endemic dimorphic fungi like Histoplasma capsulatum, and Mucormycetes continue to be the main fungal pathogens in charge of the majority of cases of serious fungal disease, despite the fact that the epidemiology of fungal diseases has significantly changed over the past few decades (Bongomin et al., 2017).

Around 11.8% of Nigeria's population is thought to get a significant fungal illness per year (Oladele and Denning, 2014). Due to congestion, poor cleanliness, and poverty, fungus infections are a significant public health issue, particularly in school-age children in rural communities (Verma and Heffernan, 2008). In Nigeria, the prevalence of fungal infections varies from community to community. These variations in fungal infection could be caused by variations in the meteorological and environmental conditions of the study sites (Joseph et al., 2022; Ogbonna et al., 1985 and Anosike et al., 2005).

Molecular docking is one of the most widely used techniques in the area of computer-aided drug design (CADD) for the discovery of new therapeutic leads (Talevi, 2018). Large drug libraries are currently being quickly annotated and analyzed using CADD, which saves a tremendous amount of energy, time, and money (Brogi, 2019; Hung and Chen, 2014, Mousavi et al., 2021).

Mitracapus hirtus L., is a plant belonging to the family Rubiaceae, it is commonly known as botton grass in English and Harwastii in Hausa, it is distributed throughout gardens, farms and fields in tropical and subtropical regions such as India, United States of America, Malaysia, Thailand, east and west African countries (Alqasim et al., 2013). Ethno botanical surveys of *M. hirtus* has shown that the plant is used for the treatment of fungal infections, skin disease such as eczema, ringworm, rashes, itching, toothache and venereal diseases, through the application of the leaf sap, rubbing leaves on skin or taken orally (Alqasim et al., 2013). Mitracarpus species have been demonstrated to have a variety of ethnomedicinal uses. Ethnopharmacologically, Mitracarpus species are utilized in folklore for a variety of purposes. M. scaber is commonly used in West African traditional medicine to treat toothaches, dyspepsia, headaches, hepatic disorders, amenorrhea, and leprosy. In Nigeria, Mitracarpus villosus is one of the plants utilized by Nupe people to heal skin problems. This is done by gathering the plant's leaves in the morning, pressing out the juice, and then applying it to eczema or skin rashes (Irobi and Daramola, 1994).

Other species of Mitracarpus have been shown to exhibit different ethnomedicinal uses, important ethnopharmacologically species of Mitracarpus are used in folklore for various purposes. M. scaber is widely used in traditional medicine in West Africa for the treatment of toothache, dyspepsia, headaches, hepatic diseases, amenorrhea and leprosy. Mitracarpus villosus is one of the plants used by Nupe people for the treatment of skin infections in Nigeria. This is done by collecting the leaves of the plant at morning hours, squeeze out the juice and then apply it to lesions of eczema or rashes on the skin (Irobi and Daramola, 1993).

Phytochemical constituents obtained from various plant sources have been shown to possess antifungal activities. Mitracarpus hirtus demonstrated better antifungal effect against differents fungal pathogens such as Candida albicans, Candida tropicalis, Aspergillus niger, Aspergillus fumigatus, Histoplasm capsulatum, Mucor sp, Microsporum gallinae, Microsporum canis, Trichophyton rubrum and Trichophyton mentagrophyte, (Abubakar et al., 2022; Bkudu et al., 2018). This work was aimed at performing in silico molecular docking and evaluation of ADMET properties of some compounds obtained from GC-MS analysis of ethyl acetate extract of M. hirtus.

Materials and Methods

Sample Collection and Identification

The samples Mitracarpus hirtus (Harwatsii) was collected at the premises of faculty of pharmaceutical sciences, Usmanu Danfodiyo University Teaching Hospital Sokoto State. It was identified at haberium Unit of the Department of Pharmacognosy and Ethnopharmacy, faculty of pharmaceutical sciences, Usmanu Danfodiyo University, Sokoto. Upon identification, a voucher number (PCG/UDUS/RUBI/002) was deposited.

The M. hirtus (leave) were shed dried, crushes into powder using pestle and motor and eventually stored at room temperature for future use. Powdered plant materials (300 g) of M. hirtus (leave) were extracted successively each with solvents of increasing polarity starting with non-polar, moderately polar and to highly polar solvent (hexane, chloroform, ethyl acetate and methanol) using maceration method for 3 days each with occasional shaking. All the extracts were evaporated in-vacuo using rotary vacuum evaporator at 40oC to afford a concentrated residue known as hexane leave extract (HLE), chloroform leave extract(CLE), ethylacetate leave extract (ELE), methanol leave extract (MLE) respectively.

Gas Chromatography-Mass Spectrometry (GC-MS) analysis

GC-MS analysis of ethylacetate extract was conducted using Shimadzu GC-MS - QP2010 PLUS. The equipment was set at the following conditions: Injector temperature – 250 oC, oven temperature – 60 oC, ion source temperature - 200 oC, interface temperature - 250 oC, pressure - 100.2 KPa, column flow - 1.61 ml/min, purge flow 5.6 ml/min and total flow time - 39.4 ml/min. Manual injection of the sample was done at a split ratio of 20:0 and the total running time was 11 min.

Molecular Docking studies

Protein Preparation

Two protein targets were used in this sudy, the targets proteins include squalene synthase (SS) and lanosterol-14 alpha demethylase (14α DM) with PDB ID: 3ASX and 5EQB. The three-dimensional structure (3D) of the proteins were retrieved from protein data bank (https://www.rcsb.org). The protein preparation was performed by cleaning all the non-standard residues and water molecules that might interfere with the proper binding of ligand within the receptor binding pocket and by adding hydrogen, assign charges for accurate energy minimization.

Ligand Preparation

The chemical compounds obtained from the results of GCMS analysis were subjected to molecular docking against some fungal molecular targets. The structure-data file (SDF) of the compounds and standard ligands i.e., 1-{4-[{4-chloro-2-[(2-chlorophenyl) (hydroxy) methyl] phenyl} (2,2-dimethylpropyl) amino]-4-oxobutanoyl} piperidine-3-carboxylic acid, flavin adenine dinucleotide (FAD) for Squalene synthase and 4-phenylimidazole for lanosterol 14-alpha demethylase were obtained from PubChem and ChamBel database (https://pubchem.ncbi.nlm.nih.gov/) respectively. The chemical structures of the compounds were prepared and converted to PDB format using Chimera 1.1413.

Molecular Docking Analysis

Molecular docking analysis were carried out to determine the binding energies of the ethyl acetate extract GCMS analysed compounds and standard ligands Using AutoDock Vina software14, against the Squalene synthase (SS), squalene epoxidase (monooxygenase) (SE) and lanosterol-14 alpha demethylase (14α DM). The produced proteins and ligands were transformed into PDBQT format. Each protein's grid box centre and grid box dimensions were taken into consideration as shown in Table 1. The PyRx software's AutoDock tools were used for molecular docking, the BIOVIA Discovery studio visualizer 2020 was used for 2D generation of the ligand-receptor interaction and Chimera 1.1413 were used for post-docking analysis.

In silico ADMET and Drug-likeness Prediction

The ADMET (Absorption, Distribution, Metabolism, Excretion and Toxicity) of the GC-MS analysed compounds from ethylacetate extract was performed using swissADME and PRotox II. By inserting the compounds' Canonical SMILES, the Molinspiration Cheminformatics free web services (https://www.molinspiration.com/cgibin/) was used to forecast the compounds' drug-likeness features.

Results

GC-MS Analysis of Ethyl Acetate Extract of M. hirtus

GC-MS analysis of the ethylacetate extract of M. hirtus revealed the presence of 30 compounds from 40 chromatogram peaks. Peaks 3, 9, 12 represent anthracene, peaks 7, 13, 18 represent glycine, peaks 26, 32 and 35 represent 3-buten-1-ol while peaks 29, 33, 36, 38 and 40 represent Cyclohexanecarboxamide. The compounds detected comprise different classes of alkaloids (quinolines, 5-(Benzyloxy)-1-methyl-1h-indole, Isocolchicine etc), hydrocarbons, alcohols, fatty acids and their derivatives and flavonoids compounds (Figure 1 and Table 1).

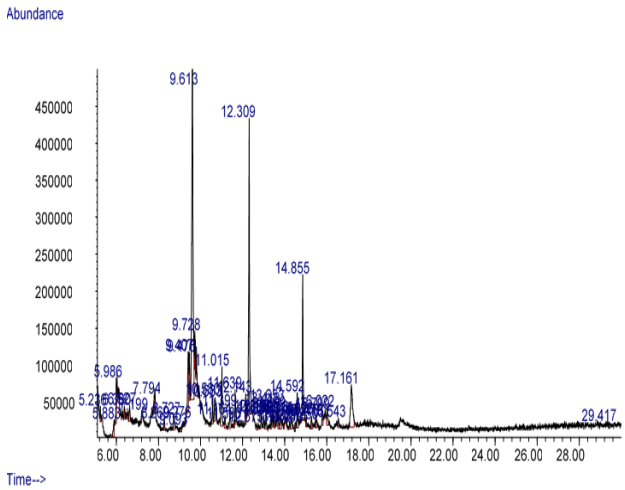

Figure 1: GC-MS chromatogram of ethyl acetate fraction of Mitracarpus hirtus leaf extract

Table 1: Chemical compounds of ethylacetate extract from GC-MS analysis

PK	R.T.	%A	%Q	Chemical compounds
1	5.236	0.36	55	N,N-Dimethyl-4-nitroso-3-(trimethylsilyl)aniline
2	5.883	0.99	64	5-(Benzyloxy)-1-methyl-1h-indole
3	6.380	0.49	53	Anthracene
4	6.627	0.82	46	5-Acetamido-6-amino-4,7-dioxo-4,7 dihydrobenzofurazan
5	7.199	0.36	43	Quinoline
6	8.269	0.42	25	2-Pyridinamine
7	8.727	0.99	27	Glycine
8	9.093	0.35	27	2-(3,5-Dimethoxyphenyl)-5-phenyl-1,3,4-oxadiazole
9	9.276	0.25	53	4-(2-(5-Nitro-2-furyl)vinyl)-2-quinolinamine
10	9.407	2.82	53	5-Amino-2-(4-chlorophenyl)-7-methyl-6-indolizinecarbonitrile
11	9.476	1.48	59	6-Chloro-3-ethyl-2-methyl-4-phenylquinoline
12	11.015	3.36	50	4-(Phenylsulfanyl)-6-(pyrrolidin-1-yl)-2,1,3-benzoxadiazole
13	11.164	0.72	35	Methyl 2-chloro-6-methoxyquinoline-4-carboxylate
14	11.593	0.31	35	3-(3-Hydroxyphenyl)-3-hydroxypropionic acid
15	11.639	1.57	47	2-Hydrazino-4,6-dimethylpyrimidine
16	12.143	1.11	43	[1-(3-Chlorophenyl)-3-trifluoromethyl-1H- pyrazolo[3,4-d]pyrimidin-6-yl]isopropyl amine
17	12.675	0.35	29	7-Hydroxy-6-methoxyisoflavone
18	12.886	0.70	38	7a,9c-(Iminoethano)phenanthro[4,5-bcd]furan-5-ol
19	13.104	0.79	37	Trans-4'-Pentyl-(1,1'-bicyclohexyl)-4-carboxylic acid
20	13.419	0.79	35	Isocolchicine
21	13.699	0.83	30	4-Hydroxyquinazoline
22	13.962	0.26	27	3,6,3',4'-Tetramethoxyflavone
23	14.014	0.36	25	N-(4-Methoxy-1,3-benzothiazol-2-yl)pentafluoropropanamide
24	14.231	0.32	22	3-(naphthalen-1-ylmethyl)-1-pentyl-1H-indole
25	14.855	0.30	23	2,4,6-Triphenylthiopyran
26	15.250	0.30	27	3-Buten-1-ol
27	15.799	0.89	35	1-(2H-1,3-Benzodioxol-5-yl)-3-(7-methoxy-2H-1,3-benzodioxol-5-yl)prop-2-en-1-one
28	16.022	1.16	16	Methyl 3-[(3-chlorophenyl)methyl]-2-cyclohexylimidazo[1,2-a]pyridine-6-carboxylate
29	16.543	0.52	35	Cyclohexanecarboxamide
30	17.161	6.05	23	2-Benzo[1,3]dioxol-5-yl-8-methoxy-3-nitro-2H-chromene

PK: Peak; R.T:Retention time; %A: Percentage area; %Q: Percentage quality

Molecular Docking Analysis

Molecular docking analysis of ethylacetate extract of *M. hirtus* compounds has shown varying degrees of binding affinities against the target proteins which includes; squalene synthase (SS), squalene epoxidase (monooxygenase) (SE) and lanosterol- 14 alpha demethylase (14α DM). The docking scores of the docked ligands are shown in table 2. The docking analysis revealed the interaction between the protein targets and the ligand molecules with the best binding free energies ranges from -10.3 to -8.0 kcal/mol and -9.3 to -7.0 kcal/mol for the compounds and the co-crystallize ligand respectively.

The seven selected compounds obtained from GC-MS analysis such as Methyl 3-[(3-chloro phenyl)methyl]-2-cyclo hexylimidazo[1,2-a] pyridine-6-carboxylate, 4-(Phenyl sulfanyl)-6-(pyro lidin-1-yl)-2,1,3-benzoxadiazole, 2,4,6-Triphenyl thiopyran, 3-(naph thalene -1-ylme thyl)-1-pentyl-1H-indole, 5-(Ben z yloxy)-1-methyl-1h-indole, 1-(2H-1,3-Benzodioxol-5-yl)-3-(7-methoxy-2H-1,3-benzodioxol-5-yl)prop-2-en-1-one and 2-Benzo[1,3]dioxol-5-yl-8-methoxy-3-nitro-2H-chromene were screened against two important fungal proteins which include squalene synthase and lanosterol 14-alpha demethylase enzymes by performing molecular docking analysis using PyRx software. The docking scores of the seven selected compounds at the active site of the two target proteins are shown in table 2.

The result of the docking analysis revealed the interaction between the selected ligands and the active site of the Squalene synthase (Figures 2 and 3); the binding score for the best pose against squalene synthase ranges from -8.6 to -10.3 kcal/mol with 2,4,6-Triphenyl thiopyran having the lowest docking score while 5-(Ben z yloxy)-1-methyl-1h-indole had the highest docking score. Most of the ligands interacted with important amino acid residues such as LEU211, GLN212, PHE54 VAL 179, PRO292 TYR179, ALA176 and MET207 while Methyl 3-[(3-chloro phenyl)methyl]-2-cyclo hexylimidazo[1,2-a] pyridine-6-carboxylate and 4-(Phenyl sulfanyl)-6-(pyro lidin-1-yl)-2,1,3-benzoxadiazole formed conventional hydrogen bonds with ASN215 and ALA176, respectively (Table 3).

The interaction of the lanosterol 14-alpha demethylase with the GC-MS analysed compounds is shown above (Figure 4 and 5). The ligands exhibited lower binding energies ranging from -8.7 to -9.7 kcal/mol. 2-Benzo[1,3]dioxol-5-yl-8-methoxy-3-nitro-2H-chromene

recorded the highest affinity (-8.7) against the target protein while 2,4,6-Triphenyl thiopyran had the lowest binding affinity. All the compounds interacted with similar amino acid residues such as GLY472 and TYR126. 1-(2H-1,3-Benzodioxol-5-yl)-3-(7-methoxy-2H-1,3-benzodioxol-5-yl)prop-2-en-1-one formed two conventional hydrogen bond with TYR140 and LYS151. Methyl 3-[(3-chlorophenyl) methyl]-2-cyclohexylimidazo[1,2-a]pyridine-6-carboxylate was found to form conventional hydrogen bonds with TYR 505, ASN501, GLY496 and GLN493. Catechin formed a hydrogen bond with TYR140 while 2-Benzo[1,3]dioxol-5-yl-8-methoxy-3-nitro-2H-chromene formed conventional hydrogen bond with ARG385 (Table 4).

Drug Likeness Parameter Prediction Output of Test Compounds

The drug likeness parameters and pharmacokinetics properties of the phytochemical constituents of M. hirtus are presented below (Table 5). All the compounds with least binding free energy exhibited molecular weight ranging from 237.30 – 382.88 g/mol, Number rotatable bond ranging from 3–6, H-bond donors were 0 for all the test compounds, H-bond acceptors from 0 – 6, iLog P values from 2.87 – 4.01, TPSA values from 4.93–82.74A2 and molar refractivity values from 74.18–107.82. The test compounds (H3,H5,H6,H7) showed zero Lipinski violation while compounds (H1,H2, H4) each had one Lipinski violation, Ghose and Egan violation was observed for H1 and H2 while compounds (H3,H4,H5,H6,H7) showed no Ghose and Egan violations, no violation was seen with all the test compounds for Veber, compounds (H1,H2), (H4) and (H3,H5,H6,H7) had two, one and zero Muegge violations respectively. An encouraging bioavailability score of 0.55 was observed for all the test compounds, compounds demonstrated a synthetic accessibility ranging from 1.7-4.45.

Pharmacokinetics Property Prediction Output of Test Compounds

All the compounds showed high GI absorption except H1, which violated Lipinski, Egan, Mugge and had low GI absorption. Compounds H1, H2 and H5 showed no BBB permeability while H3, H4, H6 and H7 had BBB permeability, only two compounds (H1 and H6) were Pgp substrates. All the ligands are potential inhibitors of CYP1A2, CYP2CI9 and CYP2C9 except for H1 which is the only non-inhibitor of CYP2C9. Compounds H2, H4 and H6 were the only non-potential inhibitor of CYP2D6 and CYP3A4. All the compounds exhibited skin permeability (LogKp) values ranging from -5.97 – -3.40 (cm/s) (Table 6).

Toxicity Prediction Output of Test Compounds

Acute toxicity prediction outcome (Table 7) revealed that all the test compounds from M hirtus showed LD50 ranging from 1190 - 4000 mg/kg and toxicity class ranging from 4 - 5 except for compounds H1, H4 and H6 whose LD50 and toxicity class could not be detected. None of the test compounds showed a tendency for hepatotoxicity and cytotoxicity. Out of the seven compounds H2, H3 and H5 are likely to be carcinogenic, mutagenic and immunotoxic while compound H7 exhibited immunotoxicity.

Table 2: Binding energies of compounds from ethylacetate extract of *Mitracarpus hirtus*

Compounds	PubChem ID	Docking Score (Kcal/mol)	
		Squalene Synthase	14α DM
N,N-Dimethyl-4-nitroso-3-(trimethylsilyl)aniline	610216	-1.0	-1.0
5-(Benzyloxy)-1-methyl-1h-indole	259196	-8.6	-7.9
Anthracene	8414	-7.8	-7.5
5-Acetamido-6-amino-4,7-dioxo-4,7- dihydrobenzofurazan	540199	-6.3	-6.8
Quinoline	7047	-5.7	-5.8
2-Pyridinamine	10439	-4.6	-4.4
Glycine	750	-3.1	-3.3
2-(3,5-Dimethoxyphenyl)-5-phenyl-1,3,4-oxadiazole	25110053	-7.9	-8.1
4-(2-(5-Nitro-2-furyl)vinyl)-2-quinolinamine	200180	-8.1	-8.2
5-Amino-2-(4-chlorophenyl)-7-methyl-6-indolizinecarbonitrile	642089	-7.9	-8.7
6-Chloro-3-ethyl-2-methyl-4-phenylquinoline	624600	-8.2	-7.7
4-(Phenylsulfanyl)-6-(pyrrolidin-1-yl)-2,1,3-benzoxadiazole	97037329	-8.7	-8.1
Methyl-2-chloro-6-methoxyquinoline-4-carboxylate	86055032	-6.9	-6.5
3-(3-Hydroxyphenyl)-3-hydroxypropionic acid	102959	-6.5	-5.8
2-Hydrazino-4,6-dimethylpyrimidine	350535	-5.6	-5.5
[1-(3-Chlorophenyl)-3-trifluoromethyl-1H- pyrazolo[3,4-d]pyrimidin-6-yl]isopropyl amine	6426293	-8.3	-9.1
7-Hydroxy-6-methoxyisoflavone	21676187	-8.1	-7.7
7a,9c-(Iminoethano)phenanthro[4,5-bcd]furan-5-ol	627072	-7.7	-8.2
Trans-4'-Pentyl-(1,1'-bicyclohexyl)-4-carboxylic acid	1712164	-7.6	-7.5
Isocolchicine	3527796	-7.7	8.2
4-Hydroxyquinazoline	135408753	-6.1	-5.6
3,6,3',4'-Tetramethoxyflavone	688812	-7.7	-7.6
N-(4-Methoxy-1,3-benzothiazol-2-yl)pentafluoropropanamide	9174266	-7.2	-8.0
3-(naphthalen-1-ylmethyl)-1-pentyl-1H-indole	56603534	-9.4	-8.9
2,4,6-Triphenylthiopyran	629781	-10.3	-9.7
3-Buten-1-ol	69389	-3.5	-3.3
1-(2H-1,3-Benzodioxol-5-yl)-3-(7-methoxy-2H-1,3-benzodioxol-5-yl)prop-2-en-1-one	42647985	-8.3	-8.9
Methyl 3-[(3-chlorophenyl)methyl]-2-cyclohexylimidazo[1,2-a]pyridine-6-carboxylate	5136003	-9.6	-9.2
Cyclohexanecarboxamide	14283	-5.0	-4.8
2-Benzo[1,3]dioxol-5-yl-8-methoxy-3-nitro-2H-chromene	624668	-8.5	-8.7
1-{4-[{4-chloro-2-[(2-chlorophenyl) (hydroxy) methyl] phenyl} (2,2-dimethylpropyl)amino]-4-oxobutanoyl} piperidine-3-carboxylic acid	CHEMBL1684827	-9.3	-
4-phenylimidazole	69590	-	-7.0
flavin adenine dinucleotide (FAD)	643975	-	-

Standard ligands: 1-{4-[{4-chloro-2-[(2 chlorophenyl)(hydroxy)methyl]phenyl} (2,2dimethylpropyl)amino]-4-oxobutanoyl}piperidine -3-carboxylic acid, for squalene synthase, 4-phenylimidazole, for lanosterol-14α demethyase

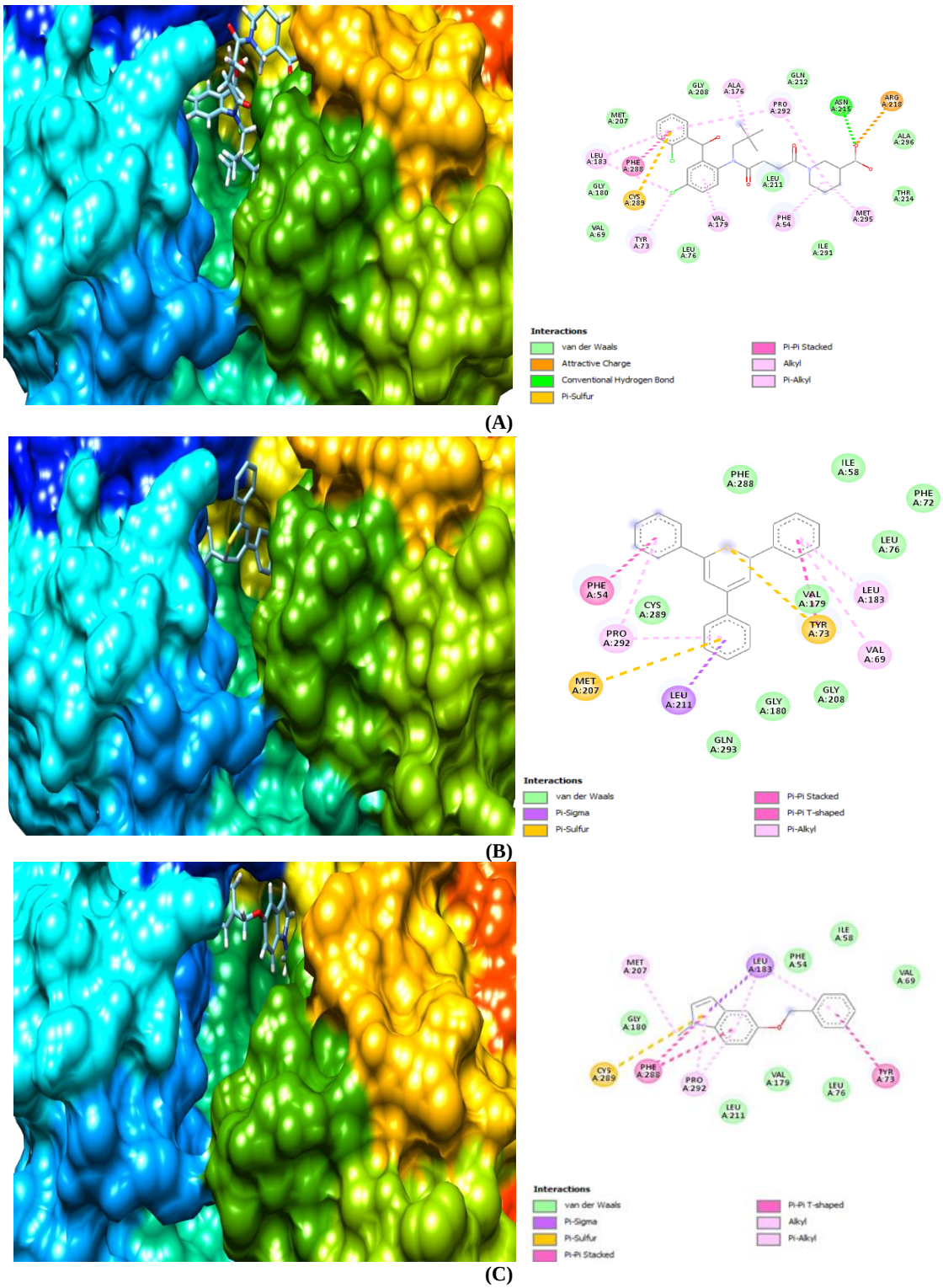

Figure 2: 3D hydrophobic surface (left) and 2D (right) views of the ligand-receptor interactions of amino acid residues of Squalene synthase with (A)1-{4-[{4-chloro-2-[(2 chlorophenyl)(hydroxy)methyl]phenyl}(2,2dimethylpropyl)amino]-4-oxobutanoyl}piperidine-3-carboxylic acid (B) 2,4,6-Triphenylthiopyran (C) 5-(Benzyloxy)-1-methyl-1h-indole .

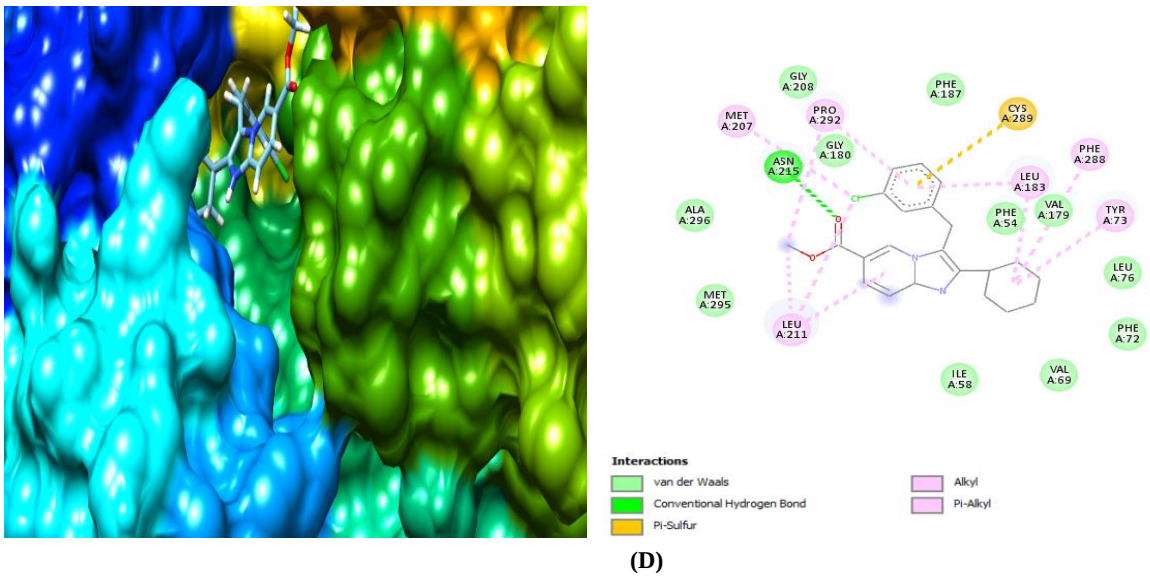

(D)

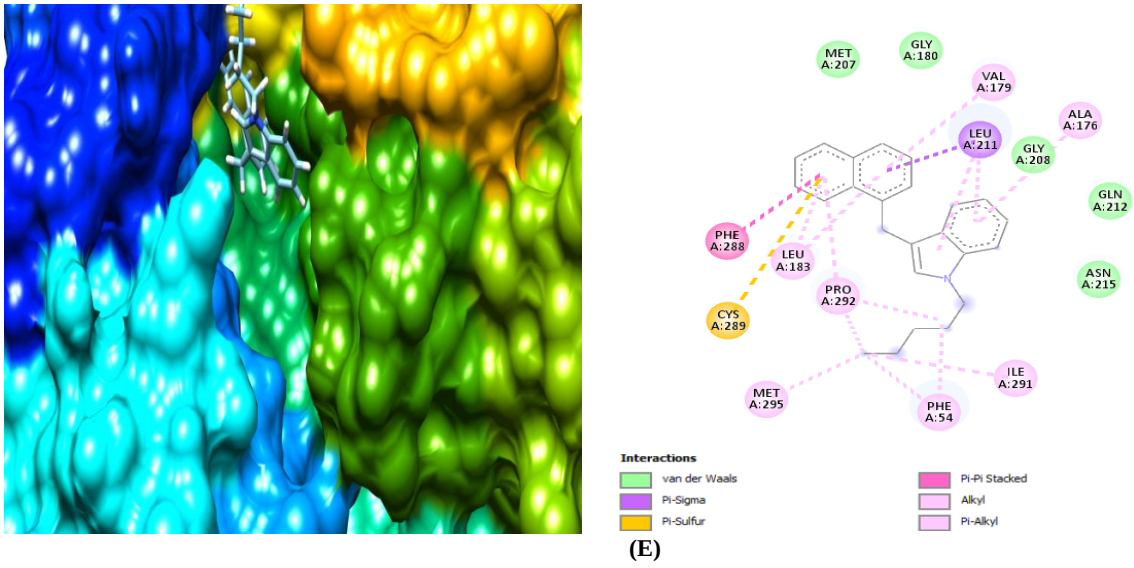

(E)

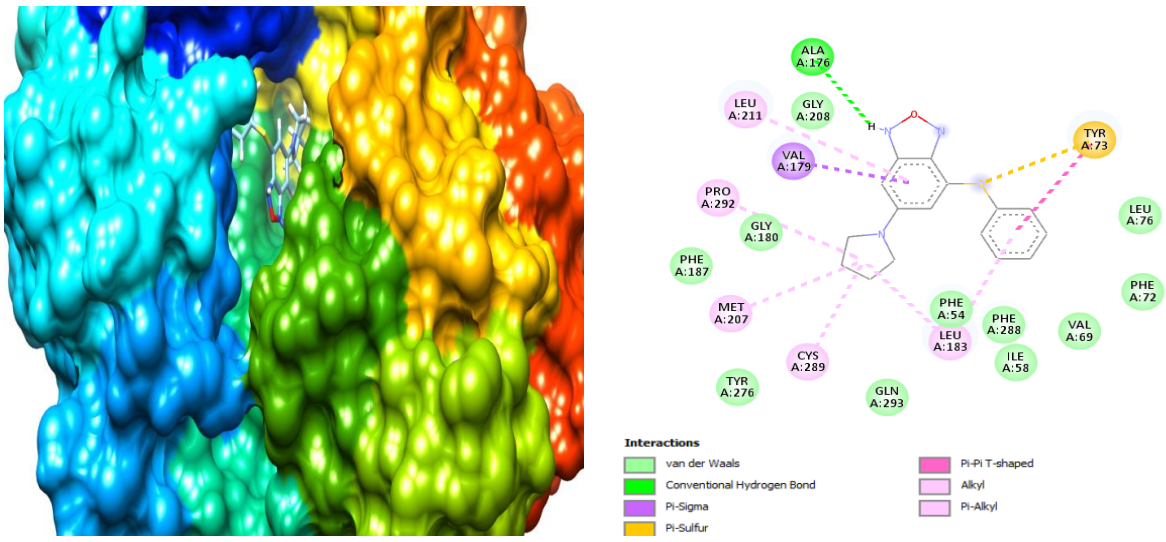

(F)

Figure 3: 3D hydrophobic surface (left) and 2D (right) views of the ligand-receptor interactions of amino acid residues of Squalene synthase with **(D)** Methyl-3-[(3-chlorophenyl)methyl]-2-cyclohexylimidazo[1,2-a]pyridine-6-carboxylate **(E)** 3-(naphthalen-1-ylmethyl)-1-pentyl-1H-indole **(F)** 4-(Phenylsulfanyl)-6-(pyrrolidin-1-yl)-2,1,3-benzoxadiazole

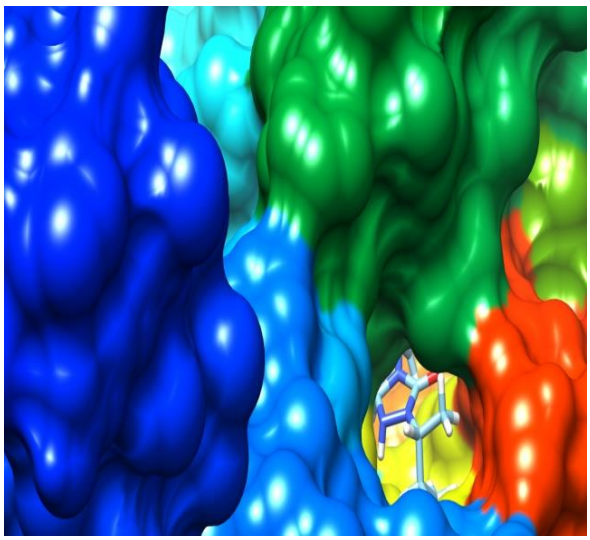

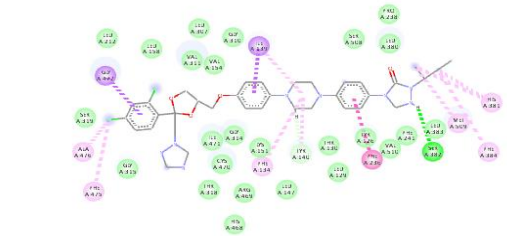

(G)

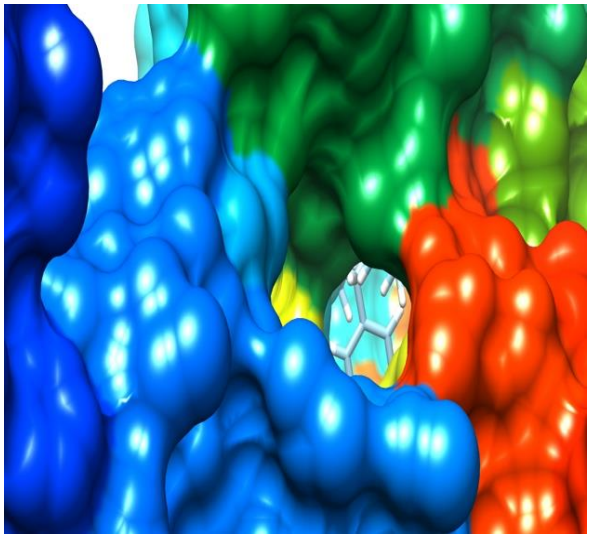

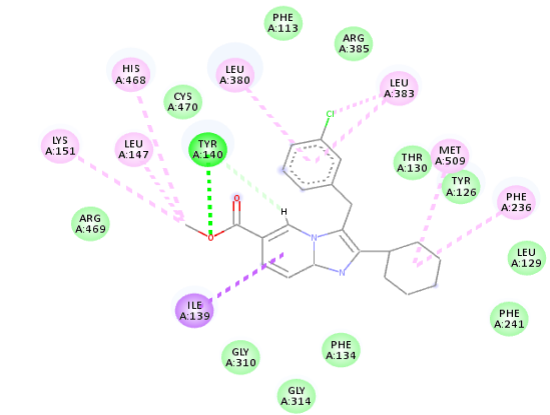

(H)

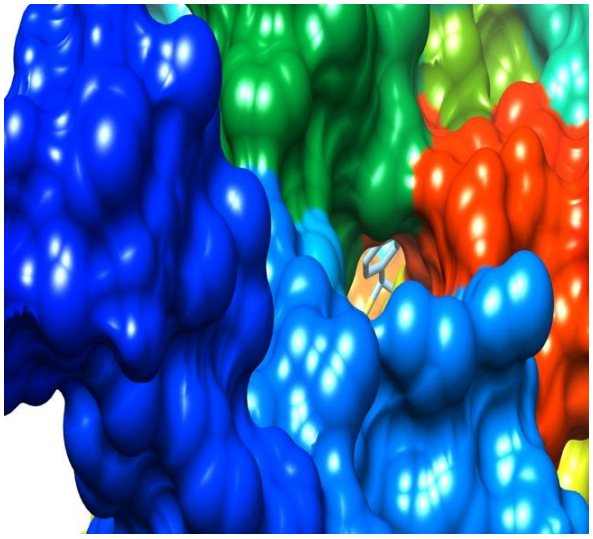

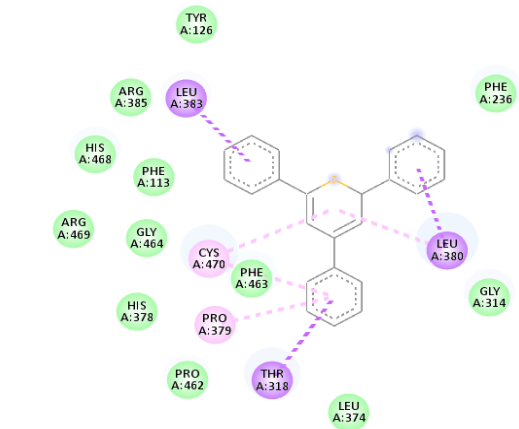

(I)

Figure 4: 3D hydrophobic surface (left) and 2D (right) views of the ligand-receptor interactions of amino acid residues of 14α demethylase with **(G)** 4-phenylimidazole **(H)** Methyl 3-[(3-chlorophenyl)methyl]-2-cyclohexylimidazo[1,2-a]pyridine-6-carboxylate**(I)** 2,4,6-Triphenylthiopyran

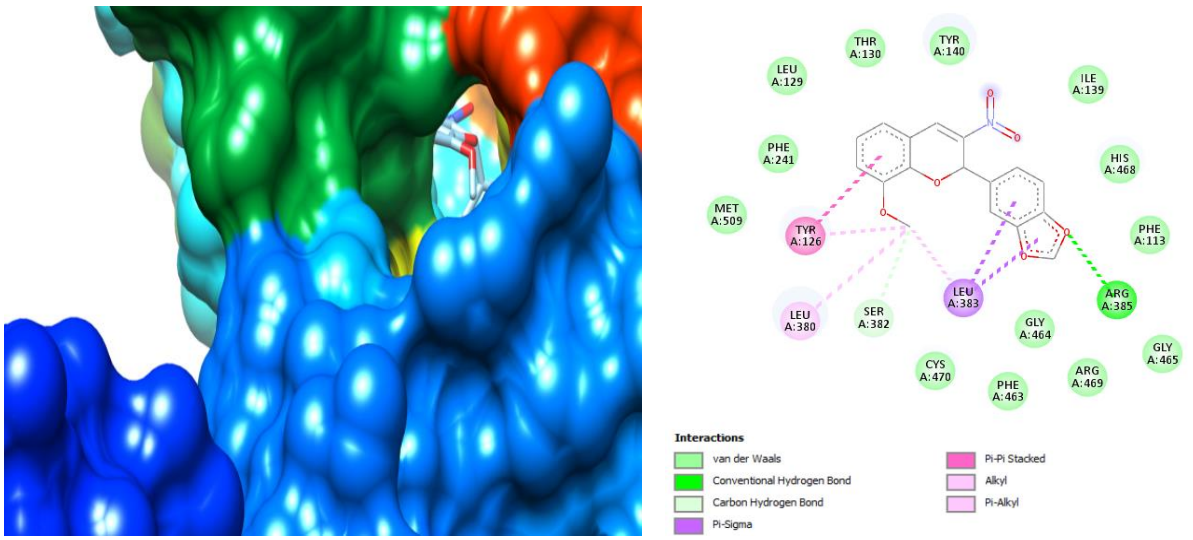

(J)

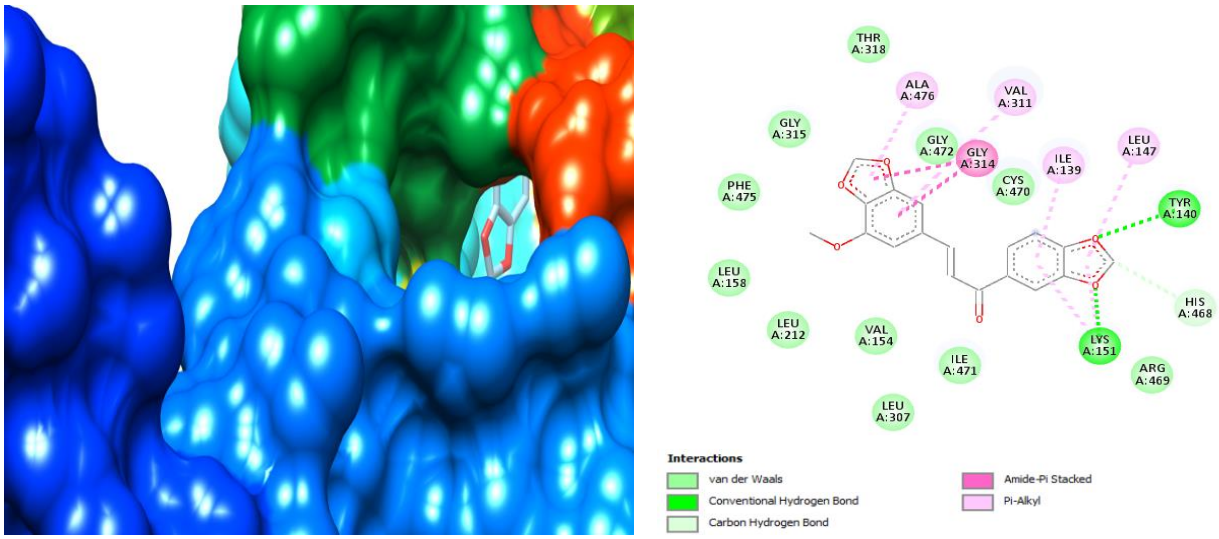

(K)

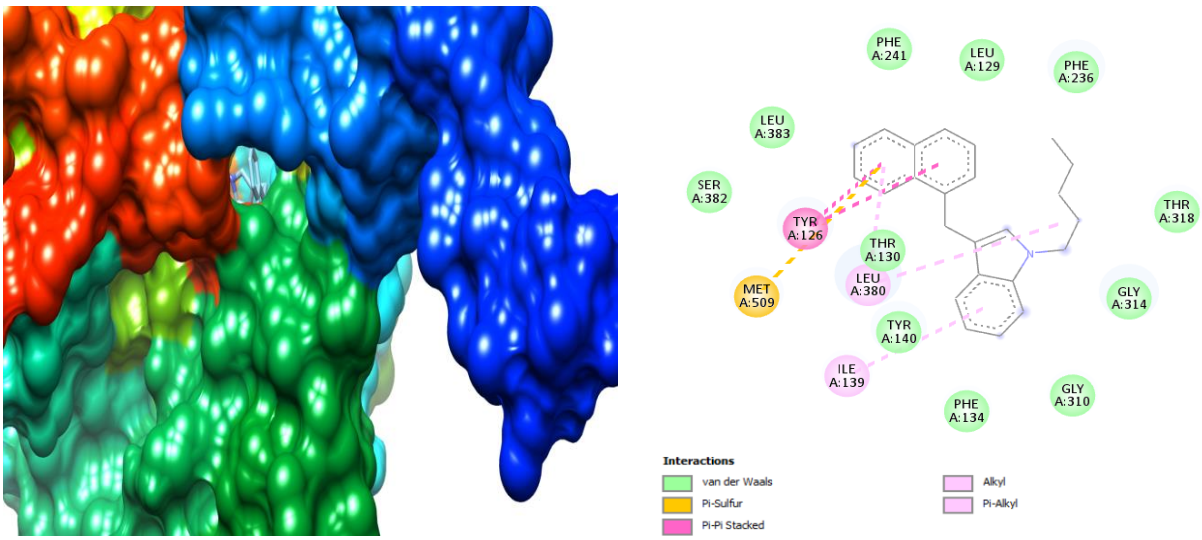

(L)

Figure 5: 3D hydrophobic surface (left) and 2D (right) views of the ligand-receptor interactions of amino acid residues of 14α demethylase with **(J)** 2-Benzo[1,3]dioxol-5-yl-8-methoxy-3-nitro-2H-chromene **(K)** 1-(2H-1,3-Benzodioxol-5-yl)-3-(7-methoxy-2H-1,3-benzodioxol-5-yl)prop-2-en-1-one **(L)** 3-(naphthalen-1-ylmethyl)-1-pentyl-1H-indole

Table 3: Ligands interaction with important amino acid residues of Squalene synthase

Compound CID	Compound Names	Interactions							
		D.S	H- bond	Pi-sulphur	Pi - sigma	Pi - Pi stacked	Pi-alkyl	Alkyl	Hydrophobic
5136003	Methyl 3-[(3-chloro phenyl)methyl]-2-cyclo hexylimidazo[1,2-a] pyridine-6-carboxylate	-9.6	ASN215	CYS289			LUE211. PRO292 LEU183	TYR73, PHE288 LEU183	PHE187,PHE54,VAL179,LEU76,PHE72,VAL69,ILE58,MET298,ALA296,GLY180, GLY208
97037329	4-(Phenyl sulfanyl)-6-(pyrolidin-1-yl)-2,1,3-benzoxadiazole	-8.7	ALA176	TYR53	VAL179	PPTS TYR73	LEU211	PRO2992, MET207, CYS289, LEU183	GLY180,GLY208,PHE187,PHE54,PHE72,LEU76,VAL69,ILE58,ALA296,PHE288,GLN293
629781	2,4,6-Triphenyl thiopyran	-10.3		TYR73, MET 201	LUE211	LUE183, VAL69	PRO 292		GLY180,GLY208,LEU76,ILE58,SPHE72,PHE288,CYS289 GLN293 ,VAL179
56603534	3-(naph thalene -1-ylme thyl)-1-pentyl-1H-indole	-9.4		CYS289	LUE211	PHE288	VAL179, ALA176, LEU183, PRO292, LEU211	ILE29, PHE54, MET295 PRO292	GLY180,GLY208,MET207,GLN212,ASN215,LEU76
259196	5-(Ben z yloxy)-1-methyl-1h-indole	-8.6		CYS289	LEU183	TYR73, PHE288	PRO292, LEU183	MET 207	GLY180,PHE54,LEU76,VAL69, LEU211, ILE58, VAL179

Table 4: Ligands interaction with important amino acid residues of lanosterol 14α demethylase

Compound CID	Compound Name	Interaction								
		D.S	H-bond	Amide -Pi	Pi-sigma	C-H	Pi-Pi stacked	Pi-alkyl	Alkyl	Hydrophobic
42647985	1-(2H-1,3-Benzodioxol-5-yl)-3-(7-methoxy-2H-1,3-benzodioxol-5-yl)prop-2-en-1-one	-8.9	TYR 140 and LYS 151	GLY 314 and LYS 151		HIS 468		LEU 147, ALA 476, ILE 139 and VAL 311		THR318, LEU212, PHE475, LEU307, LEU154, VAL154, ILE471, CYS470, GLY472, HIS468, ARG469, GLY315
5136003	Methyl 3-[(3-chlorophenyl)methyl]-2-cyclohexylimidazo[1,2-a]pyridine-6-carboxylate	-9.2	TYR 140		ILE 139			LEU 380, LEU 383	LYS151,HIS468,LEU 147, MET509PHE236	GLY310, GLY472, PHE113, PHE134, PHE241, LEU129, ARG469, ARG385, THR130, TYR126
624668	2-Benzo[1,3]dioxol-5-yl-8-methoxy-3-nitro-2H-chromene	-8.7	ARG 385	CYS 289	LEU 383	SER 382	TYR 126	TRY 383, LEU 126	LEU126,LEU383,TYR126	THR130, TYR126, LEU129, PHE241, MET509, CYS470, PHE463, GLY464, ARG469, GLY465, PHE113, HIS468
629781	2,4,6-Triphenyl thiopyran	-9.7			THR 318, LUE 380, LEU 383			PRO 379, CYS 470	LEU380	PHE236, TYR126, ARG385, HIS468, PHE113, ARG469, GLY464, HIS378, PRO462, PHE462, LEU374
56603534	3-(naphtha lene -1-yl methyl)-1-pentyl-1H-indole	-8.9					TYR 126	ILE 139, LEU 380	LEU380	GLY314, GLY310, THR318, PHE236, LEU129, PHE241, LEU383, SER382, THR130, TYR126, PHE134

Table 5: Drug likeness parameter prediction output of test compounds

Parameters	H1	H2	H3	H4	H5	H6	H7
Drug likeness							
MW	327.46	326.45	326.3	382.88	327.29	297.37	237.30
Rotatable bond	6	3	4	5	3	3	3
iLOGP	3.50	3.69	3.31	4.01	2.87	3.29	2.93
H-Bond donors	0	0	0	0	0	0	0
H-Bond acceptors	0	0	6	3	6	3	1
TPSA (A^2)	4.93	25.3	63.22	43.6	82.74	67.46	14.16
Molar refractivity	109.39	105.72	84.87	107.82	86.06	87.01	74.18
Linpiski violation	1	1	0	1	0	0	0
Ghose violations	1	1	0	0	0	0	0
Veber violations	0	0	0	0	0	0	0
Egan violations	1	1	0	0	0	0	0
Muegge violations	2	2	0	1	0	0	0
Bioavailability Score	0.55	0.55	0.55	0.55	0.55	0.55	0.55
Synthetic Accessibility	2.57	4.45	3.14	3.2	4.01	3.03	1.7

Table 6: Pharmacokinetics property prediction output of test compounds

Pharmacokinetics	H1	H2	H3	H4	H5	H6	H7
GI absorption	Low	High	High	High	High	High	High
BBB permeant	No	No	Yes	Yes	No	Yes	Yes
P-gp substrate	Yes	No	No	No	No	Yes	No
CYP1A2 inhibitor	Yes	Yes	Yes	Yes	Yes	Yes	Yes
CYP2C19 inhibitor	Yes	Yes	Yes	Yes	Yes	Yes	Yes
CYP2C9 inhibitor	No	Yes	Yes	Yes	Yes	Yes	Yes
CYP2D6 inhibitor	Yes	No	Yes	No	Yes	No	Yes
CYP3A4 inhibitor	Yes	No	Yes	No	Yes	Yes	Yes
log Kp (cm/s)	-3.4	-3.9	-5.95	-4.09	-5.97	-5.37	-5.28

H1= 3-(naphtha lene -1-yl methyl)-1-pentyl-1H-indole; H2= 2,4,6-Triphenyl thiopyran; H3= 1-(2H-1,3-Benzodioxol-5-yl)-3-(7-methoxy-2H-1,3-benzodioxol-5-yl)prop-2-en-1-one; H4= Methyl 3-[(3-chlorophenyl)methyl]-2-cyclohexylimidazo[1,2-a]pyridine-6-carboxylate; H5= 2-Benzo[1,3]dioxol-5-yl-8-methoxy-3-nitro-2H-chromene; H6= 4-(Phenyl sulfanyl)-6-(pyro lidin-1-yl)-2,1,3-benzoxadiazole; H7= 5-(Benzyloxy)-1-methyl-1h-indole

Table 7: Toxicity prediction output of test compounds

Target output	H1	H2	H3	H4	H5	H6	H7
Predicted LD50(mg/kg)	ND	1500	4000	ND	1500	ND	1190
Predicted toxicity class	ND	4	5	ND	4	ND	4
carcinogenicity	-	+	+	-	+	-	-
Hepatotoxicity	-	-	-	-	-	-	-
Mutagenicity	-	+	+	-	+	-	-
immunotoxicity	-	+	+	-	+	-	+
Cytotoxicity	-	-	-	-	-	-	-

+=Active; - = Inactive; ND= Not detected; H1= 3-(naphtha lene -1-yl methyl)-1-pentyl-1H-indole; H2= 2,4,6-Triphenyl thiopyran; H3= 1-(2H-1,3-Benzodioxol-5-yl)-3-(7-methoxy-2H-1,3-benzodioxol-5-yl)prop-2-en-1-one; H4= Methyl 3-[(3-chlorophenyl)methyl]-2-cyclohexylimidazo[1,2-a]pyridine-6-carboxylate; H5= 2-Benzo[1,3]dioxol-5-yl-8-methoxy-3-nitro-2H-chromene; H6= 4-(Phenyl sulfanyl)-6-(pyro lidin-1-yl)-2,1,3-benzoxadiazole; H7= 5-(Benzyloxy)-1-methyl-1h-indol

Discussion

Most antifungal agents in clinical usage belong to the following major classes; polyenes, echnochandins, pyrimidines analogues, azoles and allylamins, these agents are believed to target enzymes that are involves in the ergosterol biosynthesis which is the main fungal sterols required for maintaining cell membrane integrity (Satish et al., 2022).

Squalene synthase is one of the antifungal drug targets and is involve in the biosynthesis of sterols (ergosterol) catalysing the condensation of two molecules of farnesyl diphosphate to create presqualene diphosphate, followed by a rearrangement and reduction to create squalene (Dominique Sanglard, 2016). Two of the docked ligands in this study exhibited low binding energy against the target protein. These ligands are Methyl 3-[(3-chloro phenyl)methyl]-2-cyclo hexylimidazo[1,2-a] pyridine-6-carboxylate (-9.6 kcal/mol) showed conventional

hydrogen bond with ASN215 and 4-(Phenyl sulfanyl)-6-(pyro lidin-1-yl)-2,1,3-benzoxadiazole (-8.7 kcal/mol) formed conventional hydrogen bond with amino acid residue ALA176, this indicated that the former with lower binding affinities bind to the amino acid residues of the active site with stronger H-bond, as the stronger H-bonds will result in a lower energy score (Tallei et al., 2021), while the later with a bit higher binding energy may be due to formation of H-bond with a different amino acid.

Lanosterol 14-alpha demethylase is a fugal target for most of the antifungal agent especially azoles antifungal agents, it plays an important role in biosynthesis of ergosterol, it usually catalyses the conversion of lanosterol into fungal membrane called ergosterol. Three ligands demonstrated lower binding affinity against the target enzyme, these include 1-(2H-1,3-Benzodioxol-5-yl)-3-(7-methoxy-2H-1,3-benzodioxol-5-yl)prop-2-en-1-one (-8.9 kcal/mol) which formed two conventional hydrogen bond with TYR140 and LYS151, Methyl 3-[(3-chlorophenyl)methyl]-2-cyclohexylimidazo[1,2-a]pyridine-6-carboxylate (-9.2 kcal/mol) formed H-bond with TYR140 and 2-Benzo[1,3]dioxol-5-yl-8-methoxy-3-nitro-2H-chromene (-8.7 kcal/mol) formed conventional H-bond with ARG385. It could be observed that two of the ligands formed conventional hydrogen bond with similar amino acid residue TY140 suggesting that conformation and configuration of ligand molecule within the binding pocket of the protein can influence the hydrogen bonding depending on the number of H-bond donor or acceptor present in the ligand molecule or active site of the protein (Nittinger et al., 2017; Alan, 1987).

Other ligands that interacted with squalene synthase and lanosterol 14-alpha demethylase enzymes include 2,4,6-Triphenyl thiopyran (-10.3 kcal/mol), 3-(naph thalene -1-ylme thyl)-1-pentyl-1H-indole (-9.4 kcal/mol), 5-(Ben z yloxy)-1-methyl-1h-indole (-8.6 kcal/mol) and 2,4,6-Triphenyl thiopyran (-9.7 kcal/mol), 3-(naphtha lene -1-yl methyl)-1-pentyl-1H-indole (-8.9 kcal/mol) respectively, these ligands did not show any conventional hydrogen bond but exhibited lower binding energy suggesting that there exist some bond interactions such as Pi-sulphur, Pi-sigma, pi-pi-stacked, pi-pi T-shaped and pi-alkyl which contributed to lower binding score of the ligand molecules (Mhatre et al., 2021).

A Pi-sulphur, pi-alkyl, Pi-sigma, pi-pi-stacked, pi-pi T-shaped, Amide-Pi, C-H and alkyl interaction were also observed in this study, the interactions of pi-sulfur and pi-alkyl fall under the general heading of non-covalent interactions (Rakib et al., 2021), a pi-alkyl interaction, is an interaction in which a pi-electron cloud interacts with an aromatic group and an alkyl group's electron while The lone pair of the electron cloud of the sulfur atom interacts with the pi-electron cloud of an aromatic ring in the pi-sulfur interaction (De Andrade and Mendes, 2020). Charge transfer is heavily influenced by both pi-sulfur and pi-alkyl interactions and these interactions also aid in intercalating ligand molecule at the receptor binding pocket (Mhatre et al., 2021). Pi-sigma interactions provide a possible explanation for the outcome of complex stability (Bhardwaj et al., 2020). Most of the ligands in this study showed pi-sulphur and pi-alkyl interaction and it has been examined that the presence of pi-sulphur and pi-alkyl contacts in the complex, is a direction strain in the drug's backbone that normalizes the dipole moment of a drug through charge transfer with its surrounding amino acids (Arthur and Uzairu, 2019).

The seven selected docked ligands formed hydrophobic interactions with some amino acid residues of squalene synthase and lanosterol 14-alpha demethylase enzymes, Pi-cation, pi-pi and other unspecific interactions are examples of hydrophobic contacts (Nocentini et al., 2018). To maintain the proteins stability and to minimize unfavourable interactions with water, these connections (Pi-cation, pi-pi and other unspecific interactions) are crucial for protein folding (Huang and Gong, 2020). The pi-pi T-shaped interaction as observed with some of the ligands occurs when two aromatic groups engage in a T-shaped way, specifically when one ring's sideways electron cloud interacts with another ring's head-on electron cloud (Diana et al., 2020).

The drug likeness parameters of the phytochemical constituents from ethyl acetate extract of M. hirtus with lower binding free energy revealed that the molecular weight of the test ligands range from 237.30 – 382.88 g/mol, Number rotatable bond, H-bond donors, H-bond acceptors, iLog P values, TPSA values and molar refractivity values (Table 5). The test compounds (H3, H5, H6, H7) showed zero Lipinski violation while only one Lipinski violation was recorded for (H1, H2, H4) signifying that these compounds have potential of being orally bioavailable (Lipinski, 2004), Ghose and Egan violation was observed for H1 and H2 while the rest of the five compounds satisfied the Ghose and Egan rules. All the test compounds satisfied Veber's rule, two criteria as stated by Veber (Number rotatable bond ≤10 and TPSA values less than 140A2) were fund to be within the acceptable range. An encouraging bioavailability score of 0.55 was observed for all the test compounds, all the test compounds demonstrated a synthetic accessibility with H7 having the least synthetic accessibility (1.7, very easy) and H2 recording the highest synthetic accessibility (4.45, very difficult).

All the seven compounds showed high GI absorption except for compound H1 which violated some of the Lipinski, Egan and Mugge rules, human intestinal absorption permeability is a key parameter for every orally bioavailable drug candidate. The blood brain barrier is another important parameter used to determine the extent at which a molecule can cross BBB and get into the brain. In this study four out of the seven selected

compounds (H3, H4, H6 and H7) were able to passed BBB permeability criteria while compounds H1, H2 and H5 showed no BBB permeability. Efflux of xenobiotic is controlled and maintained by a cell surface protein called P-glycoprotein (Amin, 2013), if a compound is a substrate for this protein, it will remain an inhibitor of P-glycoprotein, compounds H2, H3, H4, H5, and H7 are non-substrate of p-glycoprotein and therefore are non-inhibitors of P-glycoprotein for efflux. A family of microsomal enzymes known as cytochrome P450 is involved in the metabolism of xenobiotic (Nisha et al., 2016). Five major isoforms which include CYP1A2, CYP2CI9, CYP2C9, CYP2D6 and CYP3A4 were evaluated for the test ligands' cytochrome P450 inhibition profile. All the ligands are potential inhibitors of CYP1A2, CYP2CI9 and CYP2C9 except compound H1 which is the only non-inhibitor of CYP2C9. Compounds H2, H4 and H6 were the only non-potential inhibitor of CYP2D6 and CYP3A4. All the compounds exhibited skin permeability (LogKp) values ranging from -5.97 to -3.40 (cm/s). One of the major problems with most antifungal agents especially the topical ones is their skin permeability (LogKp), thus these compounds exhibited skin permeability (LogKp) values that is within acceptable limit (Pott and Guy, 1992).

Acute toxicity prediction outcome (Table 7) revealed that the test compounds from *M hirtus* showed better LD50 and toxicity classes. Most of the selected compounds were found to be inactive for hepatotoxicity and cytotoxicity but some few compounds showed immunotoxicity carcinogenicity and mutagenicity suggesting that some of the analysed compounds could be used as potential drug candidate for the treatment of fungal infection.

Conclusions

Squalene synthase and lanosterol 14-alpha demethylase enzymes are drug targets for antifungal agents. The discovery of potential ligand molecules for these enzymes may open up new avenues for the treatment of fungal infections. We have identified some compounds in this study as potential ligands for Squalene synthase and lanosterol 14-alpha demethylase with better binding affinity than the co-crystallized ligands and their ADME toxicity profile. Molecular dynamic simulation studies will be conducted to validate the study's claim.

Declarations

Conflict of interest

No conflict of interest among the authors.

Acknowledgement

We wish to acknowledge the effort of Jaris Computational Biology Centre in providing the computational Softweres for in silico studies and Usmanu Danfodiyo University Sokoto, central laboratory for running the GC-MS analysis of the plant extract.

Consent for publications

The author approved the manuscript for publication.

Funding/support

This project is an institution-based research and was supported by the Nigerian Tertiary Education Trust Fund (TETFund) Research Projects (RP) Intervention via the Institutional Based Research Fund (IBRF) with reference number TETF/DR&D/CEUNI/SOKOTO/RG/2020/VOL. 1.

Authors' contributions

All authors contributed equally to the article.

Ethical considerations

Ethical issues (including plagiarism, misconduct, data fabrication, falsification, double publication or submission, redundancy) have been completely observed by the authors.

References

Abubakar H, Alam O, Tukur M, Muazu A, Yusuf A. Phytochemical, toxicological and in vitro antifungal studies of Mitracarpus hirtus L. Plant Biotechnology Persa. 2022; 4(2): 48-56. DOI: 10.52547/pbp.4.2.3.

Alqasim AM, Gabriel O, Is-Haq IU. Plant remedies practiced by Keffi people in the management of dermatosis. Journal of Medicinal Plants Studies. 2013; 1(5): 112-18.

Amin ML. P-glycoprotein inhibition for optimal drug delivery. Drug Target Insights. 2013; 7: 27–34. DOI: 10.4137/DTI.S12519.

Anosike JC, Keke IR, Uwaezuoke JC, Anozie JC, Obrukwu CE. Prevalence and distribution of ringworm infections in primary school children parts of Eastern Nigeria. Journal of Applied Sciences and Environmental Management. 2005; 9: 11-28. DOI: 10.4314/jasem.v9i3.17347.

Arthur DE, Uzairu A. Molecular docking studies on the interaction of NCI anticancer analogues with human Phosphatidylinositol 4,5-bisphosphate 3-kinase catalytic subunit. Journal of King Saud University - Science. 2019; 31: 1151–66. DOI: https://doi.org/10.1016/j.jksus.2019.01.011.

Bkudu AA, Odda J, Aliero JJ, Oloro J. Evaluation of antifungal activity of ethanolic crude extract of Mitracarpus hirtus plant against dermatophytes. Galore International Journal of Health Science Research. 2018; 3(1): 18–23.

Bhardwaj VK, Singh R, Sharma J, Das P, Purohit R. Structural based study to identify new potential inhibitors for dual specificity tyrosine-phosphorylation-regulated kinase. Computers in Biology and Medicine. 2020; 194: 105622. DOI: 10.1016/j.cmpb.2020.105494.

Bongomin F, Gago S, Oladele RO, Denning DW. Global and multi-national prevalence of fungal diseases – estimate precision. Journal of Fungi (Basel). 2017; 3(4): 57. DOI: 10.3390/jof3040057.

Brogi S. Computational approaches for drug discovery. Molecules. 2019; 24: 3061.

Brown GD, Denning DW, Gow NA, Levitz SM, Netea MG, White TC. Hidden killers: human fungal infections. Science Translational Medicine. 2012; 4(165): 165rv13. DOI: 10.1126/scitranslmed.3004404.

das Chagas Pereira de Andrade F, Mendes AN. Computational analysis of eugenol inhibitory activity in lipoxygenase and cyclooxygenase pathways. Scientific Reports. 2020; 10: 16204. DOI: 10.1038/s41598-020-73203-z.

Denning DW. Antifungal drug resistance: an update. European Journal of Hospital Pharmacy. 2022; 29(2): 109–112. DOI: 10.1136/ejhpharm-2020-002604.

Diana R, Caruso U, di Costanzo L, Bakayoko G, Panunzi B. A novel DR/NIR T-shaped AIEgen: synthesis and X-ray crystal structure study. Crystals. 2020; 10: 269.

Fersht AR. The hydrogen bond in molecular recognition. Trends in Biochemical Sciences. 1987; 12: 301-304. DOI: 10.1016/0968-0004(87)90146-0.

Huang H, Gong X. A review of protein inter-residue distance prediction. Current Bioinformatics. 2020; 15: 821–830. DOI: 10.2174/1574893615999200425230056.

Hung CL, Chen CC. Computational approaches for drug discovery. Drug Development Research. 2014; 75: 412–418. DOI: 10.1002/ddr.21222.

Irobi ON, Daramola SO. Bactericidal properties of crude extracts of Mitracarpus villosus (Rubiaceae). Journal of Ethnopharmacology. 1994; 42: 39–43.

Lipinski CA. Lead- and drug-like compounds: the rule-of-five revolution. Drug Discovery Today: Technologies. 2004; 1(4): 337-41. DOI: 10.1016/j.ddtec.2004.11.007.

Malwal SR, Shang N, Liu W, Li X, Zhang L, Chen C-C, et al. A structural and bioinformatics investigation of a fungal squalene synthase and comparisons with other membrane proteins. American Chemical Society Omega. 2022; 7: 22601−12.

Mhatre S, Naik S, Patravale VA. Molecular docking study of EGCG and theaflavin digallate with the druggable targets of SARS-CoV-2. Computers in Biology and Medicine. 2021; 129: 104137. DOI: 10.1016/j.compbiomed.2021.104137.

Mousavi SS, Karami A, Haghighi TM, Tumilaar SG, Fatimawali Idroes R, Mahmud S, et al. In silico evaluation of Iranian medicinal plant phytoconstituents as inhibitors against main protease and the receptor-binding domain of SARS-CoV-2. Molecules. 2021; 26: 5724.

Nisha CM, Kumar A, Vimal A, Bai BM, Pal D, Kumar A. Docking and ADMET prediction of few GSK-3 inhibitors divulges 6-bromoindirubin-3-oxime as a potential inhibitor. Journal of Molecular Graphics and Modelling. 2016; 65: 100–107. DOI: 10.1016/j.jmgm.2016.03.001.

Nittinger E, Inhester T, Bietz S, Meyder A, Schomburg KT, Lange G, et al. Large-scale analysis of hydrogen bond interaction patterns in protein-ligand interfaces. Journal of Medicinal Chemistry. 2017; 60(10): 4245-57. DOI: 10.1021/acs.jmedchem.7b00101.

Nocentini A, Bonardi A, Gratteri P, Cerra B, Gioiello A, Supuran CT. Steroids interfere with human carbonic anhydrase activity by using alternative binding mechanisms. Journal of Enzyme Inhibitory Medicinal Chemistry. 2018; 33: 1453–1459. DOI: https://doi.org/10.1080/14756366.2018.1512597

Ofonmbuk Victor J, Agbagwa O, Obakpororo E, Frank-Peterside N. The prevalence of fungal infections in six communities in Akwa Ibom State, Nigeria. African Journal of Health Sciences. 2022; 35(5): 1-7.

Ogbonna CIC, Robinson RO, Abubakar JM. The distribution of ringworm infection among primary school children in Jos, Plateau State of Nigeria. Mycopathologia. 1985; 89(2): 101-106.

Oladele R, Denning DW. Burden of serious fungal infection in Nigeria. West African Journal of Medicine. 2014; 33(2): 107-114.

Pott A Rossel, Guy RH. Prediction of skin permeability. Pharmaceutical Research. 1992; 9(5): 663-669.

Rakib A, Nain Z, Islam MA, Sami SA, Mahmud S, Islam A, et al. A molecular modelling approach for identifying antiviral selenium-containing heterocyclic compounds that inhibit the main protease of SARS-CoV-2: An in silico investigation. Briefings in Bioinformatics. 2021; 22: 1476–1498. DOI: 10.1093/bib/bbab045.

Sanglard D. Emerging threats in antifungal-resistant fungal pathogens. Frontiers in Medicine. 2016. DOI: https://doi.org/10.3389/fmed.2016.00011

Talevi A. Computer-aided drug design: An overview. Methods in Molecular Biology. 2018; 1762: 1–19.

Tallei TE, Fatima wali Y, Yelnetty A, Idroes R, Kusumawaty D, Emran TB, et al. An analysis based on molecular docking and molecular dynamics simulation study of bromelain as anti-SARS-CoV-2 variants. Frontiers in Pharmacology. 2021; 12: 2192. DOI: https://doi.org/10.3389/fphar.2021.717757

Verma S, Heffernan MP. Superficial fungal infections. In: Fitzpatrick's Dermatology in General Medicine. 2008; 1807–31. McGraw Hill Professional. 7th edition.

World Health Organization (WHO). Fungal priority pathogens list to guide research, development and public health action. Geneva: World Health Organization; 2022.